Bulletin of the Mineral Research and Exploration

http://bulletin.mta.gov.tr

Petrographic- mineralogical examination and diagenetic history of the Paleogene evaporites in Bulanık (Muş), Turkey

Pelin GÜNGÖR YEŞİLOVA[a*]

[a]*Department of Geological Engineering, Faculty of Engineering, Van Yüzüncü Yıl University, Van, Turkey*

Research Article

Keywords:
Muş, Evaporite, Diagenesis, Petrography, Minerology

ABSTRACT

Oligocene aged evaporite formations are observed in shallow sea-sabkha environments that develop in highly restricted conditions from sea in northeastern of the Muş basin. Evaporites are observed as alternated and intercalated with clastics and carbonates that developed under the control of factors such as climate, tectonism, volcanism and diagenesis. Evaporites consist of primary and secondary gypsum and minor anhydrite. In petrographic and minerologic examinations, secondary gypsum textures such as alabastrin, porphyroblastic and satin spar with anhydrite relicts, late diagenetic calcite, bitumen and bioturbation traces were detected. In SEM-EDS studies; celestine crstals, autogenic and detritic clay and quartz grains and euhedral dolomite mineral were observed. As a result of all these studies, the conditions and phases of the evaporites from the sedimentation stage to early diagenesis and late diagenesis processes of the evaporites were illuminated. Secondary gypsum consists of the origin of primary anhydrite and gypsum. From the diagenetic fluids released during the gypsum-anhydrite transformation, the late diagenetic calcite and by the interaction of the ions carried by the hydrothermal solutions to the basin with the groundwater were formed the celestite. Stream activity in the basin was determined by the presence of detritic minerals in gypsum minerals.

Received Date: 10.05.2019
Accepted Date: 22.05.2019

1. Introduction

The Muş Basin is an intermontane basin, which remains among ancient massives and contains the marine and terrestrial Paleogene sediments, in eastern Turkey. During the Oligocene period, the northeastern parts of the basin started to become shallow and the lagoons, lakes and sabkhas occasionally replaced with the sea in these restricted marine conditions (Şen et al., 2011). The best known of these basins are marine coastal sabkhas (Warren and Kendall, 1985) and shallow hypersaline environments (salt or lagoon: Orti Cabo et al., 1984; Rosell et al., 1998). In restricted basins in the study area, due to arid climatic conditions and high evaporation, the carbonate, clastic and evaporitic deposits were formed. These deposits were spread over the areas until mud flats. The evaporite formation in coastal sabkhas can be affected from factors such as; marine activities, groundwater, the position of groundwater table; sediments formed in the environment, climate and topography. The solution entry, which will release evaporite in the coastal sabkha can be provided both from the sea and groundwater (Kendall, 1978). The current similar formations to coastal sabkhas in the region are the shores of Abu Dhabi, Egypt, South Australia and North Africa in the Arabian Gulf (Perthuisot, 1980; Warren, 1982). In shallow water evaporitic environments (such as lagoons), the paleo-temperature, microbial activity and the salinity effect

Citation info: Güngör Yeşilova, P. 2020. Petrographic- mineralogical examination and diagenetic history of the Paleogene evaporites in the Bulanık (Muş). Bulletin of the Mineral Research and Exploration 162, 83-92. https://doi.org/10.19111/bulletinofmre.569619

* *Corresponding author: Pelin GÜNGÖR YEŞİLOVA, yesilovapelin@gmail.com*

affect the diagenetic processes (especially mineral substitutions). One example to the lagoon where these conditions occur can be given in Brazil (Vasconcelos and Mckenzie, 1997). In addition, the lagoon-sabkha environment in which similar conditions were formed was developed in the southwestern Sivas basin Tuzhisar Formation (Yeniköy and Küllü Members) and Erzurum-Aşkale sub-basins (Gündoğan et al., 2005; Abdioğlu et al., 2015). The evaporite-containing section reflecting these environments is located near Sıradere Village of Bulanık district of Muş (Figure 1). The Upper Cretaceous granitoid unit consists of the basement of the evaporitic unit. The evaporitic units are successively overlain by; Lower Miocene reefal limestones, Upper Miocene clastics, Upper Pliocene volcanoclastic and clastics and Quaternary alluvials (Figure 1). Since these evaporitic rocks are highly affected by the Miocene compressional tectonics, diagenesis and volcanism in the region, it will be quite interesting to define and solve the sedimentary structures, textures, lithofacies and diagenetic stages (dissolution, recrystallization, volumetric shrinkage, substitution, cementation and volatilization) of the sedimentary structures and textures developed on those rocks. So far, stratigraphic, oil and mapping studies have heavily been carried out in the study area and its surroundings (Birgili, 1968; Dinçer, 1969; Ünal, 1970; Soytürk, 1973; Sakınç, 1982; Göncüoğlu and Turhan, 1983; Şaroğlu, 1986; Akay et al., 1989; Sancay et al., 2006; Hüsing et al., 2009). Therefore, this study aims to determine the diagenetic processes and stages of these by field observations and to have an idea about the environmental conditions (pH, temperature, salinity, solution input and type, amount of detritic material) by means of petrographic and mineralogical studies.

2. Material and Method

This study was conducted in the form of field and laboratory studies. In field studies, the measured stratigraphic section, facies analysis and systematic sampling studies were carried out within field observations. For petrographic and mineralogical studies, more than 50 samples were collected from sections in horizontal and vertical directions where the facies are best observed in the measured stratigraphic sections. Evaporite samples were prepared in Thin

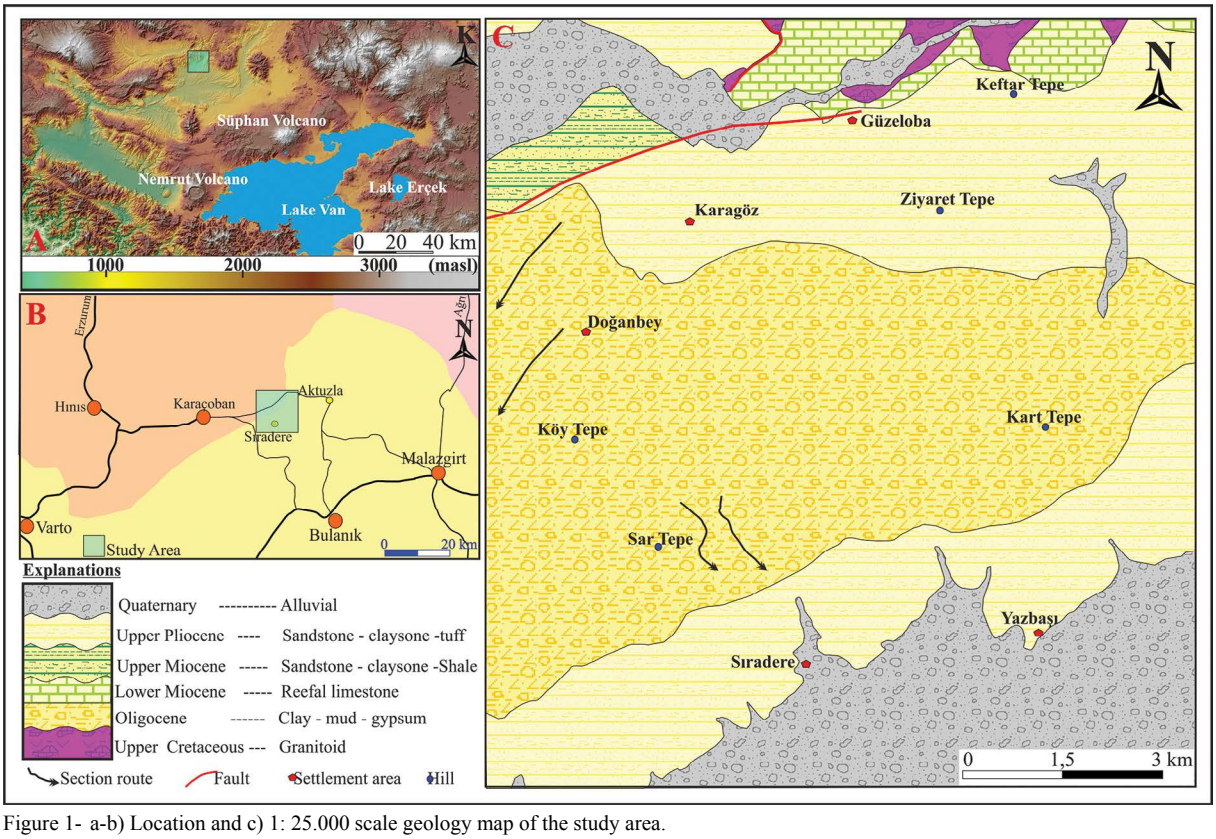

Figure 1- a-b) Location and c) 1: 25.000 scale geology map of the study area.

Section Laboratory of the Dokuz Eylül University for petrographic thin sections. Cutting, polishing and thinning processes were performed respectively in optical microscopic studies. The cutting process was performed on oil-based machine. As evaporite (gypsum, anhydrite) samples are quickly affected from temperature change when they are heated, the bonding process was carried out without heating. After the samples were left to dry, the method of cold bonding was used by hardening them 10-15 sec. under ultraviolet light utilizing the Loctite 358 adhesive. In order to see the evaporite samples more clearly, the thinning process was performed using emeries ranging between 400-800 microns then they were examined under polarized microscope. Scanning Electron Microscopy (SEM-EDS) study on 20 evaporite samples was carried out at İzmir Katip Çelebi University for the determination of some mineralogical and micro textural properties. Within the scope of the study, natural-graded crush type and polished section samples prepared for research were coated with Au-Pd, and examined and photographed on Zeiss 6060 model SEM microscope.

3. Findings and Discussion

3.1. Sedimantological and Petrographical Studies

For the sedimentological investigations in the study area, different lithofacies and sedimentary structures (folds, undulations, ripple structures) ranging from bottom to top was determined by taking measured stratigraphic sections from different areas where evaporite sequences are well observed (Figure 2). Then, petrographic thin section studies were carried out on these systematically collected samples. The measured stratigraphic sections show the depositional environments developing from lagoon-sabkha to mud flats formed by fluctuations in water levels and multiple transgression-regression processes. This evaporitic section is approximately 250 m and is composed of primary and secondary gypsum and minor anhydrites. These evaporites are occasionally interlayered and intercalated with clastic rocks such as carbonate, marl, clay, mudstone and sandstone (Figures 2 and 3a-b). All these are evidences of shallow water environmental conditions (Schreiber et al., 1976).

Secondary gypsums encountered in all sections are observed as laminated, banded, nodular, nodular

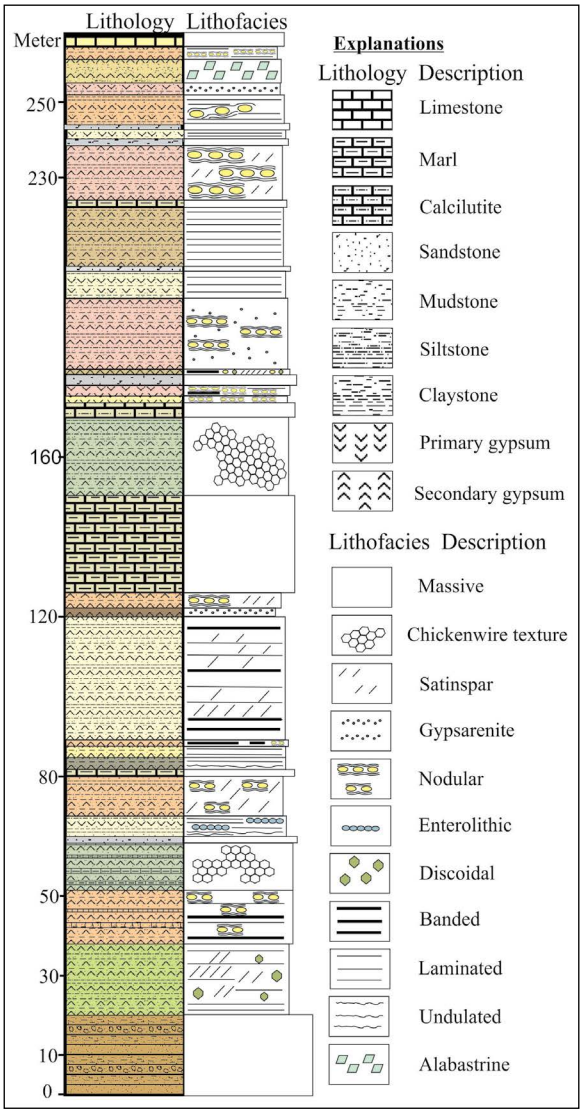

Figure 2- Generalized measured stratigraphic section of the evaporite sequence.

banded, massive and gypsum facies formed first by anhydration then transformation into secondary gypsum (gyps-arenite, selenitic, discoidal) or by the hydration of primary anhydrite (Figure 2). The selenitic primary gypsums are transparent, bright and have excellent cleavages (Figure 3c). It is observed in mudstones and are euhedral to semi-euhedral, with clear twinnings in petrographic thin sections (Figure 3d). The primarily formed gyps-arenites are dark gray, massive, sand-sized gypsums formed by dissolution and recrystallization of selenitic gypsums (Figure 3e). The ripple mark and cross-bedding morphology are evident in these gypsums. Arenitic gypsum texture in petrographic thin sections manifests itself as floating clastic grains in clay matrix (Figure 3f).

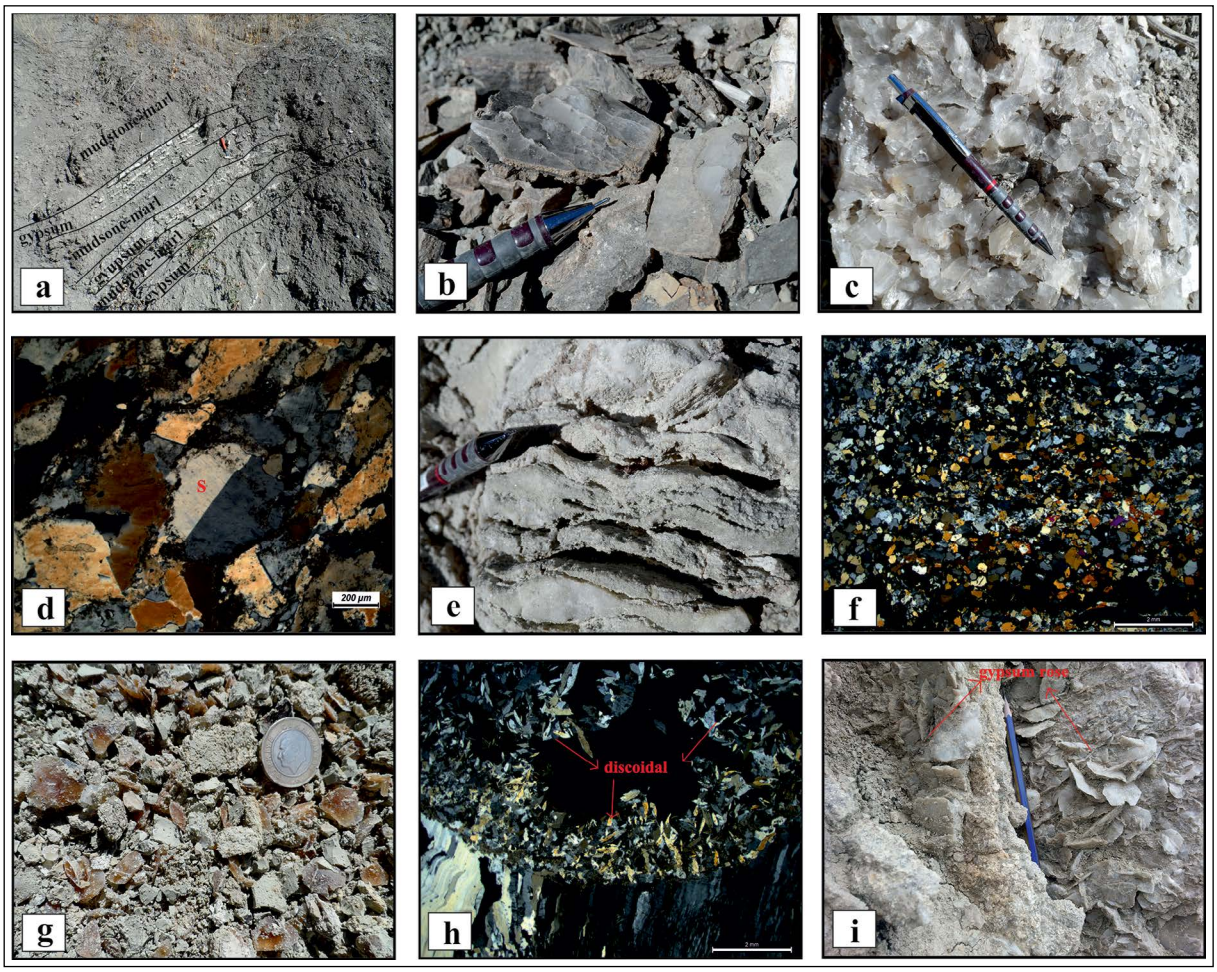

Figure 3- Sedimentological and petrographical images of primary evaporitic lithofacies. a) Mudstone-marl level alternating with gypsum, b) selenitic gypsum with claystone intercalations, c) cleavage of perfectly transparent selenitic gypsum, d) simple twinning in primary gypsum (S), e) clastic gypsum arenite, f) gypsum arenite texture (cross nicol polarizing microscope), g) brown discoidal gypsum with in mudstones, h) discoidal gypsum replaced to mudstones (cross nicol polarizing microscope) and i) cream colored gypsum rosettes.

Discoidal primary gypsums are observed as crack fill or spear head in mudstone, which range between 0.5 mm and 5 cm in size and vary from white to brown depending on the organic matter content (Figure 3g). These gypsums are observed as substituting gypsum formations replacing the carbonate matrix in petrographic studies (Figure 3h). Gypsums occur in the regression process due to the humic acid-rich groundwater within mud flats. Humic acid is a type of acid, which the bacteria produce microbially under reducing environmental conditions. Then, depending on the increase in temperature and salinity, they form gray gypsum rosettes. These roses vary in size from 0.5 cm to 4 cm.

Massive secondary gypsums have white-cream colored, occasionally gray anhydrite interbands (Figure 4a). In nodular and micro-nodular secondary lithofacies, the diameters of nodules vary between 1-20 cm and sometimes contain chicken wire, enterolithic structures and exhibit diagenetic characteristics that show replacing growth feature within the clay-carbonate matrix (Figure 4b-c-d). In petrographic thin sections the rod-like prismatic anhydrite lats, which replace with micritic matrix in early diagenetic phase in and around the nodules, are observed (Figure 4e). In addition, the areas of bituminization reflecting the reducing environment conditions are observed around the nodules (Figure 4f). The anhydrite lats growing in unconsolidated sediment combine by the effect of temperature and salinity to form anhydrite nodules. These nodules then turn into secondary gypsum in late diagenesis. This lithofacies was generally deposited with laminated secondary gypsums consisting of

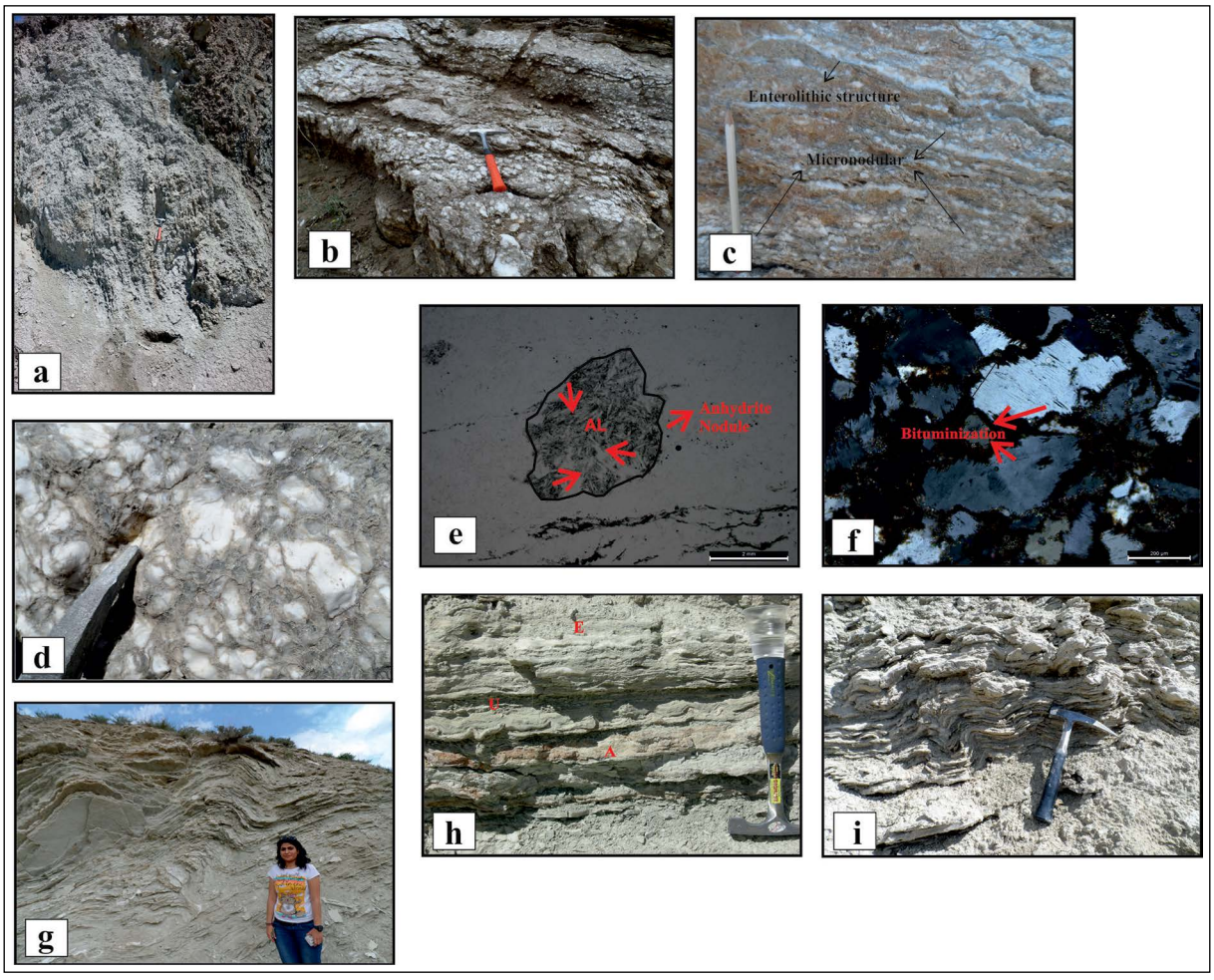

Figure 4-Sedimentological and petrographical images of secondary evaporitic lithofacies. a) Massive gypsum, b) nodular gypsum, c) gypsum containing micronodular and enterolithic structures, d) sedimentary structure showing chicken-wire texture, e) primary prismatic anhydrite lats (AL) within the micritic host sediment, these lats merge into anhydrite nodules in early-to-late diagenesis. f) bituminous areas around nodular gypsum, g) folds to the deformed version due to tectonism within these secondary gypsum, h) enterolithic (E) undulated (U) and alteration levels (A) in laminated gypsum and i) microfolds levels in laminated gypsum.

clayey, carbonated laminated between 0.1 cm and 10 cm. In laminated gypsums, the enterolithic folds, microfolds, creep structures, undulations and alteration interbands are observed (Figure 4g-h). These units to be observed together can be shown as an evidence of transition from lagoon to the coastal sabkha (Hardie and Eugster, 1971). Laminated gypsums are observed in petrographic thin sections as folded and undulated microcrystalline gypsum laminations (Figure 4i). Massive, nodular and laminated lithofacies consists of alabastrine, porphyroblastic, sutured restricted porphyroblastic gypsum textures, and anhydrite relicts (Figure 5a). This is a proof that the previous mineral is anhydrite. Alabastrine texture is seen as a fine-grained texture, which has indefinite, interlocking and undulating extinction in grain boundaries (Figure 5b). Porphyroblastic texture is generally observed with medium to coarse grained, alabastrine texture and the effect of dissolution and recrystallization processes in thin sections is easily observed (Figure 5b). The sutured boundaries in porphyroblastic, secondary gypsums (Figure 5c) indicate that they were formed earlier than alabastrine gypsums (Abdioğlu et al., 2015). Satin spar gypsums observed in both the field observations and thin sections were formed due to the effect of sediment load, hydraulic pressure and dissolution during the transformation of minerals to each other and placed in the form of cutting layers between the cracks or in vertical position (Figure 5d). The hydration channels in petrography are observed in such a way that it has been filled by these gypsums and sometimes as folded along their long axes (Figure

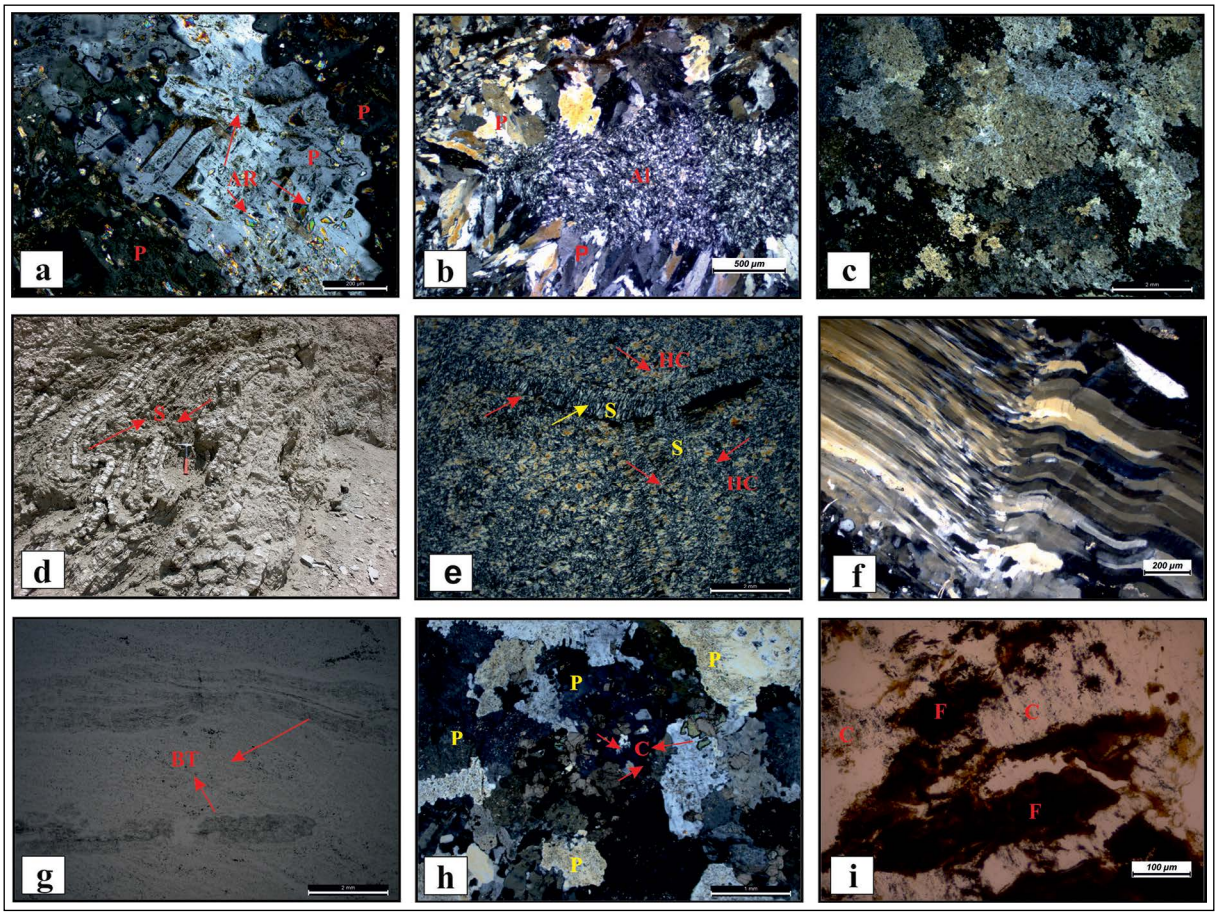

Figure 5- Petrographic images of evaporitic lithofacies. a) Primary anhydrite relicts (AR) in porphyroblastic gypsum (P), (b) alabastrin (Al) and porphyroblastic gypsum (P) textures, c) sutured-bounded porphyroblastic gypsum, d) satin-spar gypsum (S) that fill mud cracks in gypsum, e) fibrous satin-spar gypsum (S) filling the hydration channels (HC), f) curved satin spar gypsum along longaxes. g) traces of bioturbation in laminated microcrystalline gypsum (BT), h) late diagenetic calcite (C) formations in late diagenesis replacing the surface with porphyroblastic (P) secondary gypsum and i) Fe-oxidation (F) and carbonation zones (C) in gypsum.

5e-f). In addition, the bioturbition structures were encountered reflecting some foreshore environments in laminated gypsums showing micro crystalline, alabastrine texture (Figure 5g). In addition, the euhedral, semi-euhedral and anhedral calcite grains and dolomites are frequently observed and calcites are observed as replaced secondary gypsums in the late diagenetic phase (Figure 5h-i).

3.2. Mineralogical Studies

In order to identify some unidentified minerals and textures in petrographic studies, the Scanning Electron Microscope (SEM-EDS) analyses from mineralogical examinations were carried out from different evaporitic lithofacies. As a result of these studies, it was determined that minerals accompanying gypsum and anhydrites were calcite, dolomite, celestine, some clay and siliciclastic grains. Euhedral, hexagonal crystalline dolomite and clay grains are scattered in primary gypsums (Figure 6a). Gypsums are accompanied by some smectite, clay minerals and quartz grains in the syn-sedimentary process. Smectite minerals break away in spaces among nodules and exhibit corn-grain texture and curly appearances (Figure 6b). The euhedral, primary calcite mineral occasionally spreads in these clays (Figure 6b). Parallel laminated, banded and folded gypsum laminations are often observed with the effect of tectonism (Figure 6c). In addition, the siliciclastic authigenic quartz grains are planar surface and are observed in the form of scattered butterfly wings among gypsum crystals (Figure 6d). In addition, white, subhedral to euhedral tabular celestine show

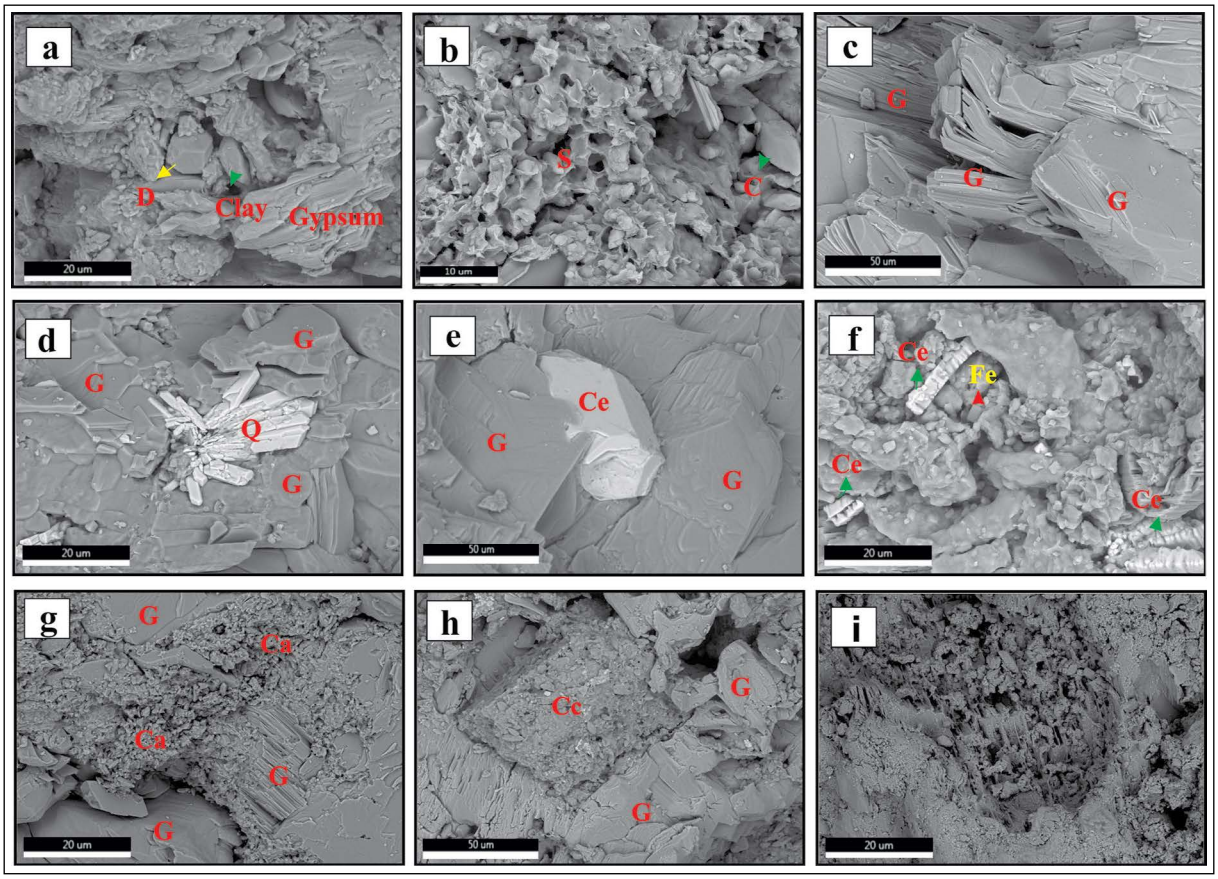

Figure 6- SEM images of evaporitic rocks. a) Euhedral hexagonal dolomite crystal (D) and clay grains during sedimentation with gypsum, b) curly textured smectite group clays (S) and euhedral calcite (C) in gypsum, c) folds and bends in laminated gypsum (G), d) scattered grains of autogenic quartz (Q) in the gypsum (G), e) celestine (Ce) grains replacing gypsum (G) in late diagenesis, f) semi-euhedral-euhedral celestines (Ce) andeuhedral feldspar (Fe) dispersed with in gypsums, g) late diagenetic carbonation (Ca) in gypsum (G), h) calcite coatings (Cc) on gypsum (G) and i) bacterial texture in gypsum.

itself as distributed in secondary gypsums (Figure 6e-f). These grains were replaced by secondary gypsums in late diagenesis. In addition, the late diagenetic carbonations, traces of alteration, calcite coatings and detritic clasts accompany gypsums (Figure 6f-g-h). In some gypsums, the textures showing the bacterial activity were determined (Figure 6i).

3.3. Diagenetic History of the Evaporites

As a result of sedimentological, petrographic and mineralogical studies, the diagenetic history of evaporites in the study area was enlightened (Figure 7). According to this, the calcite is the first mineral that was formed during sedimentation in the basin. Later, it turned into dolomite in very early diagenesis with the circulation of Mg rich waters and increasing salinity and temperature (Önalgil et al., 2015). The primary gypsum crystals (such as; discoidal and gyps-arenite) are formed in displaced character in dolomitic sediment and then turn into anhydrite with increasing salinity in syn-sedimentary to very early diagenetic stage by being dehydrated (Figure 7). These gypsums, which are buried due to sedimentation and lose water in them, were subjected to volumetric shrinkage, compressed and cemented. At this time, the prismatic anhydrite lats growing in the unconsolidated dolomitic sediment during the early diagenesis phase prior to compression were grown and formed anhydrite nodules. As the sedimentation is continuous and pressure increases, these nodules were combined to form chicken-wire and enterolithic structures. These compressed anhydrite nodules at depths were rehydrated in late diagenesis by interacting with groundwater and/or meteoric waters as they exhume under the influence of pressure or tectonism and were transformed into secondary gypsums (alabastrine, porphyroblastic textures) (Figure 7). The primary anhydrite lats in

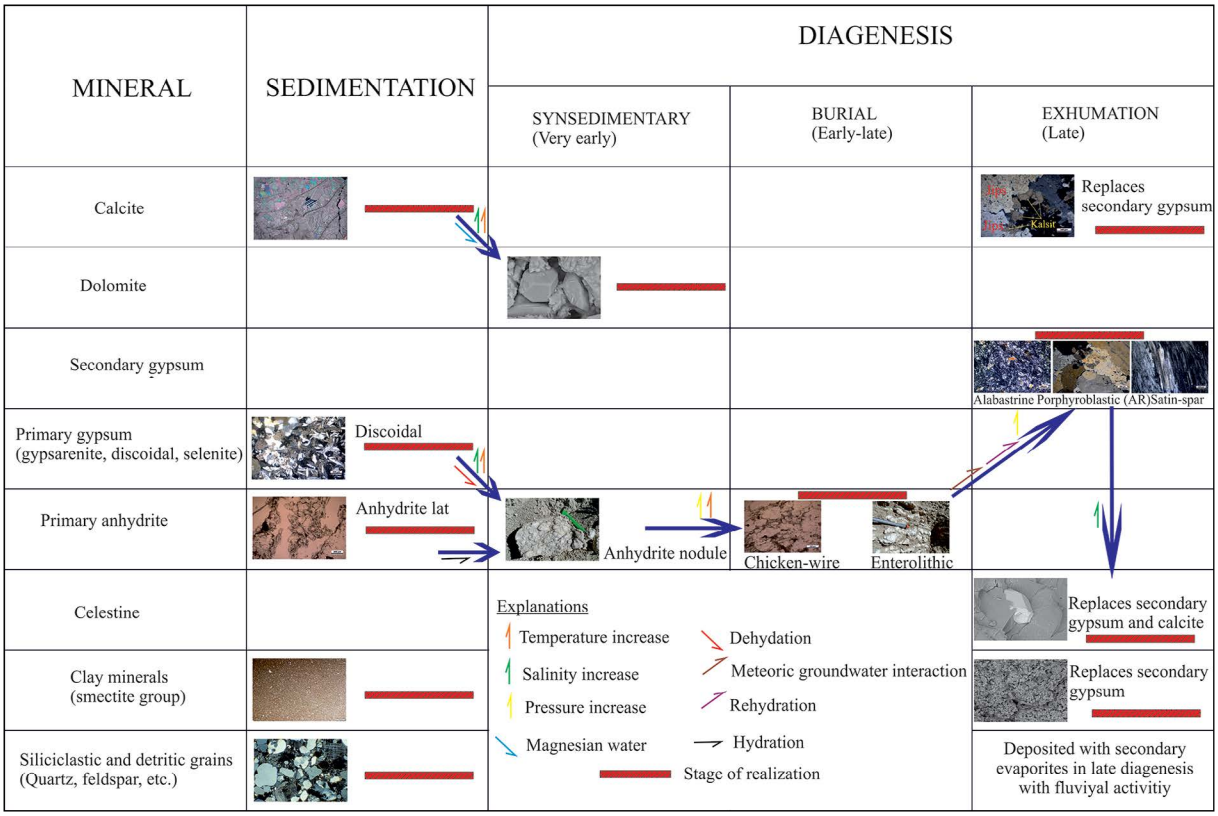

Figure 7-Diagram showing the diagenetic history of evaporites.

micritic carbonate with the presence of anhydrite relicts in secondary gypsums indicate that gypsums were originated from the primary anhydrite (Kinsman, 1966). The satin spar gypsum filling the hydration channels as an indicator of volumetric increase during the gypsum-anhydrite transformation were formed on the surface in late diagenesis (Shearman et al., 1972) (Figure 7). In addition, celestines may have formed during epigenetic hydration events (released diagenetic fluids) that occurred during anhydrite-gypsum transformation (Shearman, 1964; Rosell et al., 1998; Gündoğan et al., 2005; Orti et al., 2014). The dissolved Sr^{2+} in the evaporitic units may have been obtained by the circulation of meteoric or groundwaters, which mixed with Sr-rich fluids like seawater and hydrothermal solutions related to volcanic activity in the region. Sr ions obtained in this way settle in the crystal lattices of gypsums, they replace Ca^{2+}, and lead to the formation of celestine (Ceyhan, 1996). In addition, the diagenetic calcite was replaced by the secondary gypsum lithofacies from the waters released during mineral transformation in the last diagenetic phase. The stream activity in syn-sedimentary and late diagenetic phase caused a large amount of detritic material to be transported into the basin and precipitated with evaporites (Figure 7).

4. Conclusion

Massive, laminated, nodular, discoidal, gyps-arenite and selenitic lithofacies defined by sedimentological and petrographical studies and chicken-wire, enterolithic structures, ripple formations, folds and undulations including the sedimentary structures show that this basin is an isolated shallow water environment extending to the lagoon-sabkha and mud flats. This basin is under the influence of seasonal water level changes (repeating lithofacies in measured stratigraphic sections), tectonism (formation of sedimentary structures), arid climate (presence of smectite mineral) and reducing conditions (bituminization and bacterial activity).

Some of the secondary gypsums were formed by the hydration of anhydrite and the others were formed by the dehydration of primary gypsum and rehydration. Mineralogical studies showed that the minerals accompanying these evaporites were carbonate,

celestine, authigenic clay and siliciclastic grains and the deformation structures were formed on evaporites by the effect of carbonations in the evaporites in late diagenesis, tectonism and diagenesis.

High pH (>7.5), salinity, temperature, organic matter and long arid climatic conditions led to the formation of various and smooth gypsum crystals. In addition, it was noticed that the most important factors in the transformation of minerals in diagenetic processes (early-late) were temperature, pressure, salinity, the interaction with surface and groundwater, diagenetic and hydrothermal solutions. Under these circumstances, the texture, sedimentary structure and mineralogical compositions of the evaporites determined as a result of all these studies showed that they underwent diagenetic stages such as volumetric shrinkage, cementation, replacement, substitution, dissolution and recrystallization.

As a result of these studies, the diagenetic development of the gypsums in the study area was formed as follows; the calcite, dolomite, primary gypsum and anhydrite were transformed to each other in the syn-sedimentary-early diagenetic phase respectively. Later on; the porphyroblastic secondary gypsum, alabastrine secondary gypsum, satin spar gypsum, celestine and calcite minerals were formed in the late diagenetic phase at or near the surface.

Acknowledgements

This study was carried out within the scope of Van Yüzüncü Yıl University Scientific Research Project (No: 2014-MİM-B082). I would like to thank Çetin Yeşilova and Mustafa Açlan for their contributions during field studies. I would also like to thank İbrahim Gündoğan for his assistance in petrographic and mineralogical studies.

References

Abdioğlu, E., Arslan, M., Aydınçakır, D., Gündoğan, İ., Helvacı, C. 2015. Stratigraphy, mineralogy and depositional environment of the evaporite unit in the Aşkale (Erzurum) sub-basin, Eastern Anatolia (Turkey). Journal of African Earth Sciences 111, 100–112.

Akay, E., Bıkan, E., Ünay, E. 1989. Stratigraphy of The Muş Tertiary Basin. Bulletin of The Mineral Research and Exploration 109, 59–76.

Birgili, Ş. 1968. Muş bölgesi 1/25000 ölçekli J48 d3, d4 ve Muş K47 b2 paftalarının detay petrol etüdü hakkında rapor. Maden Tetkik ve Arama Genel Müdürlüğü Rapor No: 1707, Ankara (unpublished)

Ceyhan, F. 1996. Occurence and Origin of Celestite Mineralization Around Sivas. PhD, Cumhuriyet University, Sivas (unpublished).

Dinçer, A. 1969. Muş K47-b3 paftasının jeolojisi. Maden Tetkik ve Arama Genel Müdürlüğü Rapor No: 1997, Ankara (unpublished)

Gündoğan, İ., Önal, M., Depçi, T. 2005. Sedimentology, petrography and diagenesis of Eocene-Oligocene evaporites: the Tuzhisar formation, SW Sivas Basin. Turkish. Journal Asian Earth Science 25, 791–803.

Göncüoğlu, C.M, Turhan, N. 1983. Geology of the Bitlis Metamorphics Belt. Geology of Taurus Belt, International Symposium, 26–29 September 1983, Ankara.

Hardie, L.A., Eugster, H.P. 1971. The depositional environment of marine evaporites: A case for shallow, clastic accumulation. Sedimentology 16, 187–220.

Hüsing, S.K., Zachariasse, W.J., Van Hinsbergen, D.J., Krijgsman, W., İnceöz, M., Harzhauser, M., Mandic, O., Kroh, A. 2009. Oligocene Miocene basin evolution in SE Anatolia, Turkey: constraints on the closure of the eastern Tethys gateway. Geology Sociecty London Special Publication 311, 107–132.

Kendall, A.C. 1978. Facies Models 12: Subaqueous Evaporites. Geoscience 5, 124–138.

Kinsman, D.J.J. 1966. Gypsum andanhydrite of recentage, Trucial Coast, Persian Gulf. Proceedings of the 2nd International Salt Symposium, Cleveland, Ohio, 302–326.

Önalgil, N., Kadir, S., Külah, T., Eren, M., Gürel, A. 2015. Mineralogy, geochemistry and genesis of the modern sediments of Seyfe Lake, Kırşehir, Central Anatolia, Turkey. Journal Afican Earth Science 102, 116–130.

Ortí, F., Pueyo, J.J., Geisler-Cussey, D., Dulau, N. 1984. Evaporitic sedimentation in the coastal salinas of SantaPola (Alicante, Spain). Revista del Instituto de Investigaciones Geologicas 38/39, 169–220.

Orti, F., Perez-Lopez, A., Garcia-Veigas, F., PerezValera, F. 2014. Sulfate isotope compositions ($\delta^{34}S$, $\delta^{18}O$) and strontium isotopic ratios ($^{87}Sr/^{86}Sr$) of Triassic evaporites in the Betic Cordillera (SE Spain). Revista de la Sociedad Geológica de España 27, 79–89.

Perthuisot, J.P. 1980. Sites et processes delaformationd' evaporites dans la natureactuelle. Bull. Cent. Rech.Explor. Elf-Aquitaine 4, 207–233.

Rosell, L., Orti, F., Kasprzyk, A., Playa, E., Peryt, T.M. 1998. Strontium geochemistry of primary gypsum: Messinian of southeastern Spain and Sicily and Badenian of Poland. Journal Sediment. Res. 68, 63–79.

Sakınç, M. 1982. Mollababa-Uruman (Muş ili) yöresinin jeolojisi biostratigrafisi ve paleontolojisi. İstanbul Yerbilimleri 3, 1-2.

Sancay, R.H., Batı, Z., Işık, U., Kırıcı, S., Akça, N. 2006. Palynomorph, foraminifera, and calcareous nanoplankton biostratigraphy of Oligo-Miocene sediments in the Muş Basin, Eastern Anatolia, Turkey. Turkish Journal Earth Science 15, 259–319.

Schreiber, B.C, Freidman, G.M, Decima, A., Schreiber, E. 1976. Depositional environments of upper Miocene (Messinian) evaporite deposits of the Sicilian Basin. Sedimentology 23, 729–760.

Shearman, D.J. 1964. Recent celestine from the sediments of theTrucial Coast of the Persian Gulf. Nature 202 (4930), 385 – 386.

Shearman, D.J., Mossop, G.D., Dunsmore, H., Martin, M. 1972. Origin of gypsum veins by hydraulic fracture. Trans. Inst. Min. Metall. 81, 149–155.

Soytürk, N. 1973. Murat Havzası jeolojisi ve hidrokarbon imkânları. TPAO, Arama Grubu Rap. No. 791, Ankara (unpublished).

Şaroğlu, F. 1986. Doğu Anadolu'nun neotektonik dönemde jeolojik ve yapısal evrimi. Maden Tetkik ve Arama Genel Müdürlüğü Rapor No: 244, Ankara (unpublished).

Şen, S., Antoine, P.O., Varol, B., Ayyıldız, T., Sözeri, K. 2011. Giant rhinoceros Paraceratherium and other vertebrates from Oligocene and Middle Miocene deposits of the Kağızman-Tuzluca Basin Eastern Turkey. Naturwissenschaften 98, 407–423.

Ünal, A. 1970. Muş bölgesi 1/25 000 ölçekli Erzurum J47-C4 Muş K47-b4-cl-e2 paftalarının detay petrol etüdü. Maden Tetkik ve Arama Genel Müdürlüğü Rapor No: 4754, Ankara (unpublished).

Vasconcelos, C., McKenzie, J.A. 1997. Microbialmediation of modern dolomite precipitation and diagenesis under anoxic conditions (LagoaVermelha, Rio De Janeiro, Brazil). Journal of Sedimentary Petrology 67, 378–390.

Warren, J.K. 1982. The hydrological setting, occurrence and significance of gypsum in late Quaternary salt lakes in South Australia. Sedimentology 29, 609–637.

Warren, J.K., Kendall, C.G.S.C. 1985. Comparison of sequnces formed in marine sabkha (subaerial) and salina (subaqueas) settings-modern and ancient. American Association of Geology Bulletin 69, 1013–1023.